

Anisotropic Si Etching Condition for Preparing Optically Smooth Surfaces

Minoru Sasaki, Takehiro Fujii and Kazuhiro Hane

Department of Mechatronics & Precision Engineering, Tohoku University,
Aza Aoba 01, Aramaki, Aoba-ku, Sendai 980-8579, Japan

(Received September 30, 2002; accepted January 14, 2003)

Key words: surface roughness, {110} surface, anisotropic etching, microcavity

A combination of dry and wet anisotropic Si etching has been found to be useful for preparing hexagonal holes having smooth sidewall surfaces. The dry etching defines the main shape, and the subsequent short-time wet etching smoothens the sidewall of the {110} surface. The etchant used is made up of ethylenediamine pyrocatechol and water. The surface roughness is quantitatively investigated for improving the sidewall smoothness. The angular alignment accuracy between the pattern and the crystallographic orientation is found to be important. The triangular etching pit obtained by the dummy etching is used for confirming the crystallographic orientation. The surface roughness of <20 nm Ra is repeatedly obtained. The solid polymer dye microcavity laser is fabricated as a replica of the Si structure obtained. The lasing spectra from microcavities show the higher Q value.

1. Introduction

Optical components are one of the major applications of micromachining. Examples are elements for coupling between optical fibers or between fibers and semiconductor lasers. The reflection mirror is required to be smooth. The polishing technique is effective only for the top substrate surface. The small micro-optical system frequently requires 45° or 90° mirrors prepared on the substrate. In such cases, the surface quality depends on the etching technique. Although the Si{111} surface is easily obtained by the wet anisotropic etching, it is not convenient for constructing the optical setup. For setting the {111} surface at 45°, the wafers cut at 9.7° off the [100] axis are sometimes investigated.⁽¹⁾ The vertical {111} surface can be obtained from the (110) wafer.⁽²⁾ Other than the {111} surface, {100} surfaces can be introduced as the vertical sidewalls by aligning the mask

E-mail: sasaki@hane.mech.tohoku.ac.jp

opening along a $\langle 100 \rangle$ orientation.⁽³⁾ A cubic corner on a (100) wafer is achieved by the delicate balance of the corner compensation with the etching ratio.⁽⁴⁾ When the $\{110\}$ surface is considered, a 45° angle can be obtained on the (100) substrate.⁽⁴⁾ The 90° angle can also be obtained on (111) and (100) substrates. The hexagonal or the tetragonal optical paths can be set using a set of $\{110\}$ surfaces. Up to now, we have demonstrated the Si mold having such side surfaces, and the solid polymer dye microcavity laser is prepared as the replica of the Si mold.^(5,6) The total internal reflection at each sidewall confines the light inside the cavity generating the round-trip path. The surface roughness is an important factor deciding the laser oscillation. The rough sidewall causes optical loss, disturbing the total internal reflection. The technique for smoothening the reflection surface becomes the key for obtaining a good microcavity.

In our previous experiments, the reproducibility was poor. Although the fabrication process is the same, the threshold power for the laser oscillation changes from run to run. Sometimes lasing is not achieved. This can be attributed to the lack of control of some important factors, which have a close relation with the surface roughness. In this study, the surface roughness of the sidewall surface is investigated for improving the sidewall smoothness and the microcavity replica.

2. Materials and Methods

Figure 1 shows the process sequence for preparing the cavity mold. This has been previously presented, but is included here for completeness and for clarifying the improvements. The starting Si(111) wafer is oxidized and patterned as a hexagonal array. Since the deep reactive ion etching (RIE) forms the vertical holes, the hexagonal pattern is manually aligned so that the sidewalls will be $\{110\}$ surfaces. The as-etched sidewalls have a significant roughness, which comes from the isotropic etching in the cycle of the used pulsed plasma etching technique (3rd step in Fig. 1). This randomness tends to increase with the etching depth. The anisotropic wet etching is then applied (4th step in Fig. 1). The etchant is 115°C ethylenediamine pyrocatechol and water (EDP), which is a mixture of anhydrous ethylenediamine (280 ml), pyrocatechol (90 g), deionized water (90 ml), and pyrazine (2 g). Since the substrate is Si(111), the wet etching mainly proceeds in the lateral

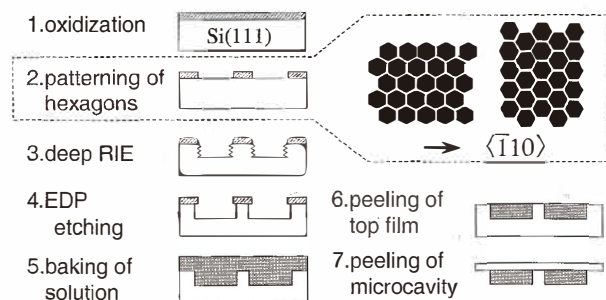


Fig. 1. Process sequence for preparing microcavities.

directions attacking the sidewalls. The etching rate of EDP has relative minima at the $\{110\}$ surfaces in addition to the $\{111\}$ surfaces.⁽⁷⁾ Since the dry-etched sidewalls are aligned close to $\{110\}$ surfaces, a short-time etching (typically a few minutes) removes the sub-micrometer corrugation, which corresponds to the surfaces having the larger etching rate. Since six $\{110\}$ surfaces (e.g., $(\bar{1}10)$, $(\bar{1}01)$) are intrinsically perpendicular to the substrate (111) surface and the angles between them are accurately 120° , the hexagonal prism shape can be prepared. The optical alignment is obtained automatically. Figure 2(a) shows the typical Si mold having $\{110\}$ sidewall surfaces. Figure 2(b) is the mold having orthogonal $\{211\}$ surfaces. Although the $\{211\}$ surface is incidentally obtained, the smooth microcavity can be obtained from this mold. Therefore, this surface is also investigated in the following.

The microcavity replicas are prepared by filling the Si mold with a solution of the laser dye (rhodamine 6G perchlorate) and poly(methyl methacrylate) (PMMA) in the solvent. After the baking (80°C for ~ 4 h), the solidified polymer is manually peeled using adhesive tape two times. The first peeling is carried out at room temperature. Only the film on the wafer top surface is removed (6th step in Fig. 1). The hexagonal PMMA structure remains inside the Si hole, since the microcavity is tightly embedded inside. The second peeling is carried out by heating the sample up to 100°C , which is slightly under the glass transition temperature of PMMA. The microcavities are considered to become soft during the peeling process (7th step in Fig. 1). Figures 3(a) and 3(b) are cavities fabricated from the mold having the $\{110\}$ and $\{211\}$ side surfaces, respectively. The shape of the Si mold is clearly transferred to the PMMA including the minute structure on the sidewall showing the importance of the quality of the sidewall.

On the sidewall of the Si mold, there are two different structures which will disturb the mirror quality. One is the spot as shown in Fig. 4, another is the ledge described later. The spot can be considered to have a relation with the defects inside the Si matrix or the thermally induced dislocation. This sample is actually set into and withdrawn from the 1100°C furnace in ~ 20 s under an oxygen environment. The defect inside the crystal matrix

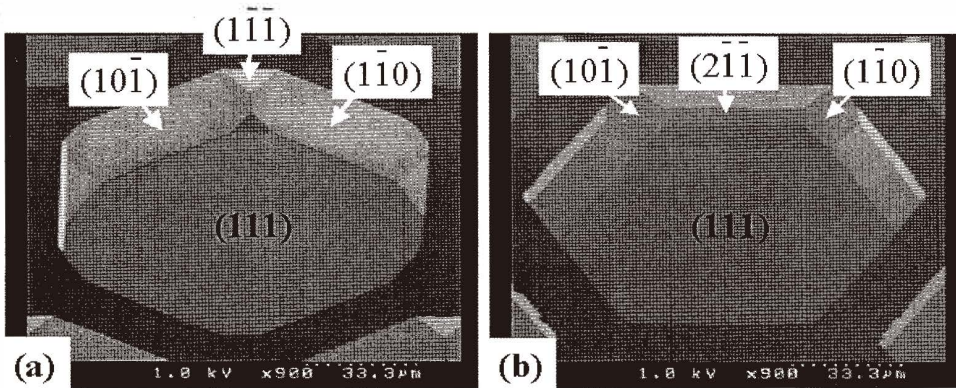


Fig. 2. Fabricated Si mold having (a) $\{110\}$ and (b) $\{211\}$ sidewalls. The mold having $\{211\}$ sidewalls has $\{110\}$ surfaces also at corners.

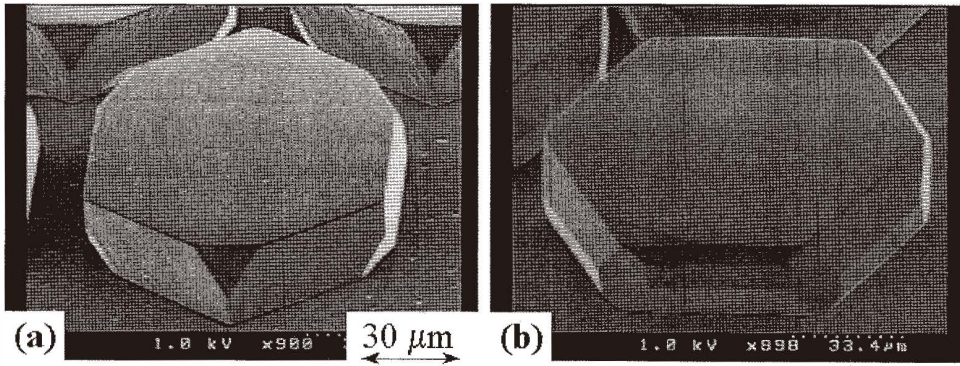


Fig. 3. Microcavity replicas prepared from the Si mold having (a) {110} and (b) {211} sidewalls.

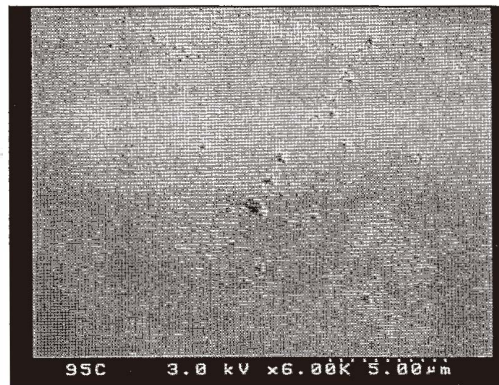


Fig. 4. Spot structure observed on {110} side surfaces.

is known to decrease by annealing under the N_2 environment. The annealing is carried out before the oxidization (1st step in Fig. 1). For selecting the surest method, the wafer is set in the oxidation furnace at room temperature, and the temperature is increased under N_2 gas flow. The annealing is performed at 1100°C for 30 min, and the oxidization is then carried out. Then, the environment is changed to a N_2 one and the temperature is decreased to room temperature. The rate of temperature decrease is less than $200^\circ\text{C}/\text{h}$. The above process decreases the number of spots down to almost zero.

For the quantitative roughness measurement using the surface profiler, the sample sidewall is required to be set horizontally. The Si flakes ($\sim 100\ \mu\text{m}$ in width, $\sim 300\ \mu\text{m}$ in depth, $\sim 3\ \text{mm}$ in length) are prepared from the 1 mm-thick Si wafer. This Si flake is manually taken from the substrate using tweezers and placed with its sidewall surface facing upward. Figure 5 shows the schematic diagram of the sample with flakes. The fabrication process is the same as that for the microcavity. Figure 6(a) is the optical micrograph of the dry etched side surface (3rd step in Fig. 1) showing the random

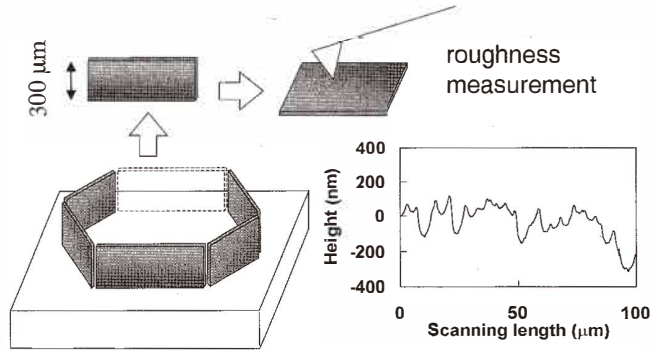


Fig. 5. Sample preparation for measuring the sidewall roughness using the surface profiler. The included graph is the typical profile obtained by scanning the stylus across ledges on {110} surfaces.

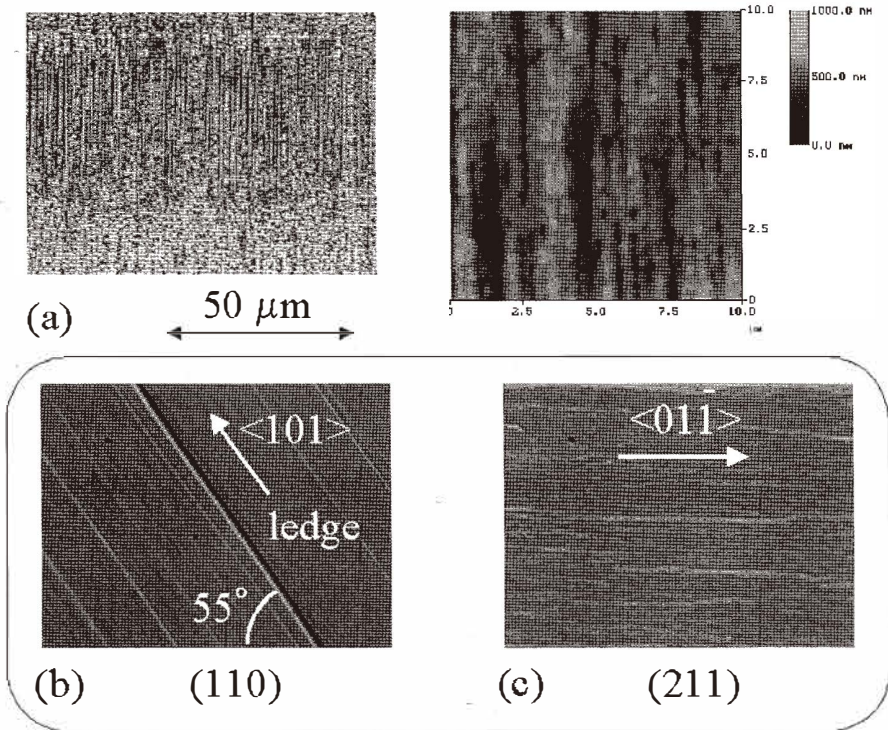


Fig. 6. Micrographs of sidewall surfaces. (a) as-dry-etched side surface, EDP etched (b) {110} and (c) {211} surfaces.

corrugation. The typical corrugation depth is $\sim 1 \mu\text{m}$ as seen from the atomic force microscope image, which corresponds to the etching depth of one cycle of the pulsed plasma etching. This random corrugation is removed by the EDP etching. Figure 6(b) shows the (110) surface. There are sharp lines of ledges whose direction is decided by the intersection between $(10\bar{1})$ and $(\bar{1}\bar{1}\bar{1})$ surfaces (see also Fig. 2(a)). The ledge line is at an angle of 55° against the (111) wafer top surface. Although the side slope of each ledge is considered to be the $\{111\}$ surface, the crosssection across ledges does not show a linear zigzag profile, but a rounded one as shown in Fig. 5. Figure 6(c) shows the (211) surface. The ledges are wavy and obscure in their contour, not showing clear regularity.

3. Results

Figure 7 is the surface roughness measured by the surface profiler (KLA-Tencor, P-15) as a function of etching time. One or two Si flakes are taken from the wafer while continuing the etching. Since the etched surface has a directional structure, the stylus is scanned across and along ledges at random positions on the Si flake. The filled and empty circles show the data obtained by scanning the stylus across and along ledges, respectively. Three different positions are measured for one condition. The scanning length is $100 \mu\text{m}$. Figure 7(a) is obtained from the $\{110\}$ sidewalls. The profile along the ledge soon

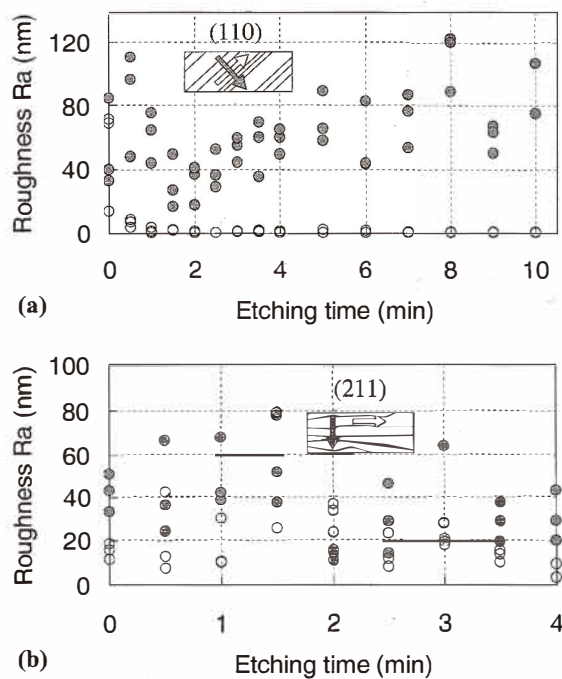


Fig. 7. Surface roughness obtained from (a) $\{110\}$ and (b) $\{211\}$ sidewalls when the orientation flat is used for the alignment.

becomes smooth. Even after the 30 s etching, the roughness is down to <10 nm Ra. The profile across ledges shows the larger roughness. The surface roughness does not decrease much showing the minimum of ~ 50 nm Ra at ~ 2 min etching time. The subsequent increase of the roughness corresponds to the increase of the ledge height with the etching time. In such a case, the obtained microcavity does not show the clear lasing peaks in the luminescent spectrum (nothing or small peaks). Figure 7(b) is the result for the $\{211\}$ sidewalls. Since the ledges on $\{211\}$ do not have a clear regularity, the stylus is scanned in the vertical and horizontal directions against the wafer top surface, which will be roughly across and along ledges, respectively. The obtained result is similar to that of $\{110\}$ sidewalls. With the large fluctuation, the roughness value does not show convergence.

It is considered that the alignment accuracy between the hexagonal pattern and the crystallographic orientation has an essential meaning for obtaining the smooth surface. The orientation flat is used as the alignment reference in the experiment of Fig. 7. The accuracy of the orientation flat is $\pm 1^\circ$. In the general anisotropic Si etching technique using a (100) wafer, the underetching is minimized by aligning the pattern to the crystallographic orientation which is cleared by the dummy etching.⁽²⁾ Also in our system, the dummy etching is carried out. Figure 8 shows the process sequence including the dummy etching. The shallow triangular pits are obtained after the etching for a few minutes as shown in Fig. 8. These etching pits can be observed over the substrate. The pits have a gathering tendency. The triangle size grows with the etching time. The time utilized for the dummy etching is typically 2 min, since a longer etching time tends to make the triangular sidelines round especially when the etchant is old. The typical triangle size is ~ 500 μm . The direction of these triangles is the same, and the sidelines correspond to the $\langle 110 \rangle$ directions. Therefore, these sidelines are used instead of the orientation flat. For the alignment, the long (~ 2 cm) straight lines are included in the mask as shown in Fig. 8. The patterning is carried out aligning these lines to be parallel to the sidelines of triangles over the wafer. Figure 9(a) depicts the surface roughness of $\{110\}$ sidewalls obtained by the

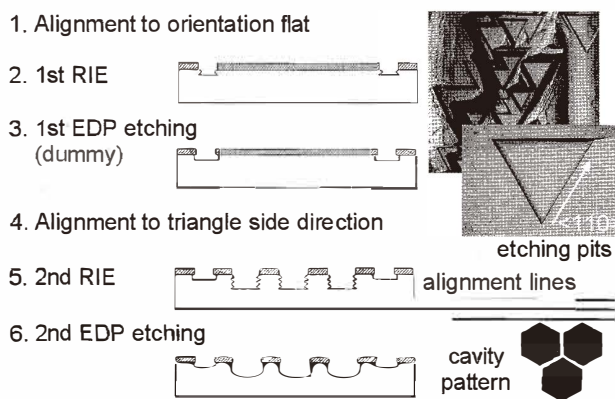


Fig. 8. Process sequence with dummy etching. The included images are etching pits obtained after the dummy etching.

above process. The roughness along ledges is constantly sub-nm Ra. The roughness across ledges decreases stably and monotonically with the etching time and reaches <20 nm Ra when the etching time is >4 min. Figure 9(b) is the result of $\{211\}$ sidewalls. Again the surface roughness stably decreases with the etching time. The roughness values along both vertical and horizontal scans reach <10 nm Ra when the etching time is >2.5 min. Notice that the etching ratio of the $\{211\}$ surface is larger than that of the $\{110\}$ surface. The above roughness value seems to be as small as for the wet etched surface. The surface roughness obtained by the well-controlled KOH etching is typically 50–100 nm Ra.^(8,9) Veenendaal et al. report that there is no microscopically smooth surface over the Si hemisphere sample after the KOH or TMAH etching.⁽¹⁰⁾

The spectrum from the cavity having $\{110\}$ sidewalls is shown in the following, since the results are similar between cavities obtained from the mold having $\{110\}$ and $\{211\}$ surfaces. The second harmonic generation light (532 nm) of a Nd:YAG laser is used with 10 ns pulses at a 10 Hz repetition rate. The emission from the microcavity is collected using the microscope objective and analyzed using a spectrometer. Figure 10 shows the spectra of the cavities prepared by the alignment method using etching pits. The EDP etching time is 4 min. As the pumping energy increases, sharp peaks increase in height and number. Compared with the previous result prepared using the orientation flat,⁽⁵⁾ the Q

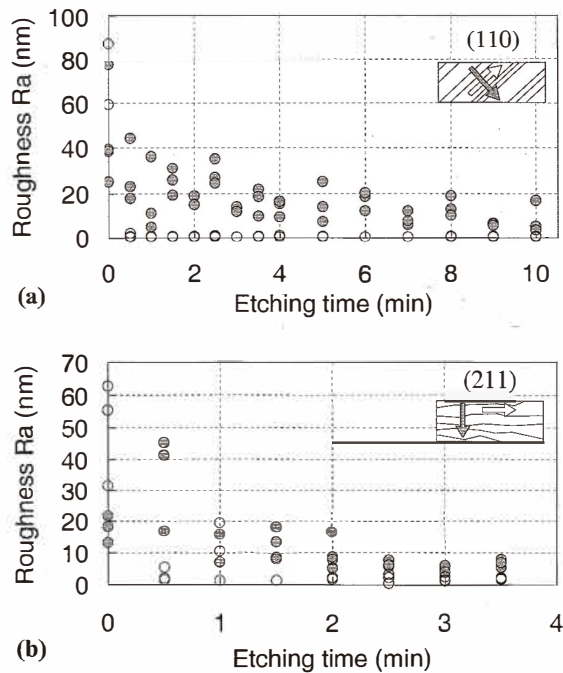


Fig. 9. Surface roughness obtained from (a) $\{110\}$ and (b) $\{211\}$ sidewalls when the etching pit is used for the alignment.

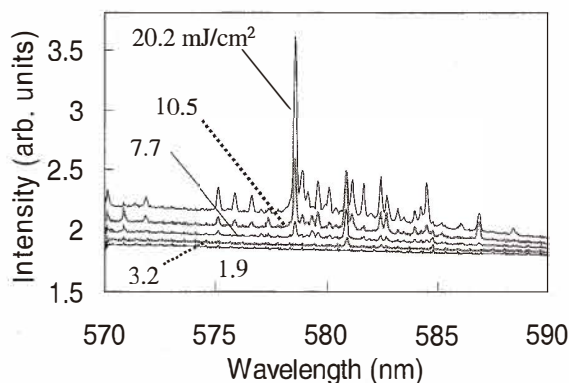


Fig. 10. Luminescence spectra of cavities prepared from the Si mold having {110} sidewalls.

value of the peak increases from ~ 1600 to $2500\text{--}4500$. The threshold power decreases from 10 to 3 mJ/cm^2 . The repeatability for obtaining the lasing peak is also improved. This can be attributed to the improvement of the sidewall quality. When the spectrum of each cavity is measured, the lasing peaks are confirmed from almost all cavities.

4. Discussion

The anisotropic etching selects specific crystal surfaces, and the Si{110} surface corresponds to the local minima of the surface free energy when the density of the dangling bonds is simply counted.⁽¹⁾ However, the etched surface generally becomes rougher with the etching time. Actually, the smoothing phenomenon is exceptional and depends on the etchant. There are reports which show that EDP yields a smoother surface compared to KOH or KOH/IPA in the other experimental systems, although the quantitative roughness value has not been measured.^(1,4) Similar etchant dependence can be seen also in the case of the etching pit. The EDP etching generates sharp triangular etching pits. On the other hand, KOH or TMAH etching generates a rounded one, which is unsuitable for defining the crystallographic direction.⁽¹⁰⁾ The absolute accuracy obtained by the etching pits is not clear at present. Seidel et al. report that the lateral underetching rate of EDP in the vicinity of the {111} surface shows a high sensitivity against the angular orientation.⁽⁷⁾ Their data implies the necessity of the 0.1° level accuracy. Since many etching pits over the substrate are used in our second alignment (4th step in Fig. 8), a 0.1° level accuracy is considered to be obtained. The inner angle of the triangle is close to 60° . The measured difference from 60° is -0.03° in the average of 20 different triangles (therefore 60 angles). This indirectly supports the accuracy of the direction of the triangle side.

Figure 11 shows the numerical density of ledges as a function of the etching time. The filled triangle and the open circle show the data when the alignments are carried out using the etching pits and the orientation flat, respectively. The decreasing tendency of the ledge density is not very clear, showing a large fluctuation from place to place. The dependence on the alignment methods is also small. It should be mentioned that counting the ledge

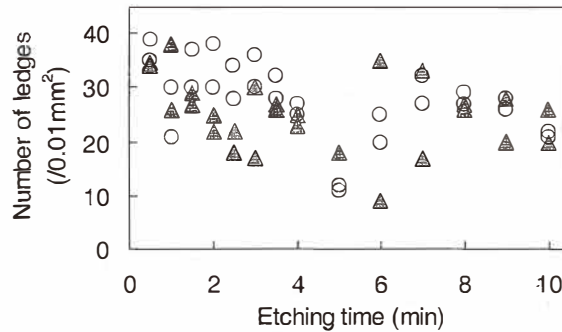


Fig. 11. Density of ledges on the {110} sidewall as a function of etching time.

number from the optical micrograph is not very quantitative. Although the image contrast is optically increased by the edge illumination mode, detection of minute ledges having only a slight contrast change (and therefore a slight angular change) is difficult by an optical microscope. The height of ledges decreases to less than 100 nm as shown in the typical crosssection in Fig. 5. Identifying the ledge from the crosssection is also difficult. Although the definition of the ledge is disputable, it is natural to consider that the described improvement of the surface roughness is mainly obtained by decreasing the height of ledges. There is a possibility that the minute distortion of the hexagonal resist pattern disturbs the decrease of the number of ledges.

Acknowledgment

A part of this work has been performed at the Venture Business Laboratory in Tohoku University.

References

- 1 C. Strandman, L. Rosengren and Y. Backlund: Proceedings of Micro Electro Mechanical Systems 1995 (IEEE catalog number 95CH35754) p. 244.
- 2 Y. Uenishi, M. Tsugai and M. Mehregany: Proceedings of Micro Electro Mechanical Systems 1994 (IEEE catalog number 94CH3404-1) p. 319.
- 3 M. Elwenspoek and H. V. Jansen: Silicon Micromachining (Cambridge University Press, 1998) Chap. 2, p.34.
- 4 Y. Backlund and L. Rosengren: J. Micromech. Microeng. **2** (1992) 75.
- 5 M. Sasaki, Y. Li, Y. Akatu, T. Fujii and K. Hane: Jpn. J. Appl. Phys. **39** (2000) 7145.
- 6 Y. Li, M. Sasaki and K. Hane: J. Micromech. Microeng. **11** (2001) 234.
- 7 H. Seidel, L. Csepregi, A. Heuberger and H. Baumgartel: J. Electrochem. Soc. **137** (1990) 3612.
- 8 M. Madou: Fundamentals of Microfabrication (CRC Press, Boca Raton, Newyork) chap. 4, p. 173.
- 9 E. D. Palik, O. J. Glembocki, I. Heard, Jr, P. S. Burno and L. Tenerz: J. Appl. Phys. **70** (1991) 3291.
- 10 E. V. Veenendaal, K. Sato, M. Shikida and J. V. Suchtelen: Sens. Actuators A **93** (2001) 219.
- 11 P. J. Hesketh, C. Ju, S. Gowda, E. Zanolari and S. Danyluk: J. Electrochem. Soc. **140**(1993) 1080.